Available online at www.sciencedirect.com
SCIENCE DIRECT®
International Journal of Heat and Mass Transfer 49 (2006) 1214–1224
International Journal of HEAT and MASS TRANSFER
www.elsevier.com/locate/ijhmt

A two-dimensional model of the kettle reboiler shell side thermal-hydraulics

Milada Pezo [a], Vladimir D. Stevanovic [b,*], Zarko Stevanovic [a]

[a] Department of Thermal Engineering and Energy, Institute of Nuclear Sciences, Vinca, P.O. Box 522, 11001 Belgrade, Serbia and Montenegro
[b] Faculty of Mechanical Engineering, University of Belgrade, Kraljice Marije 16, 11000 Belgrade, Serbia and Montenegro

Received 3 May 2005
Available online 5 December 2005

Abstract

A two-dimensional two-fluid numerical model is developed for the prediction of two-phase flow thermal-hydraulics on the shell side of the kettle reboiler. The two-phase flow around tubes in the bundle is modeled with the porous media approach. A closure law for the vapour–liquid interfacial friction is based on modified pipe two-phase flow correlations. The tube bundle flow resistance is calculated by applying to each phase stream the correlations for the pressure drop in a single phase flow across tube bundles and by taking into account the separate contribution of each phase to the total pressure drop. Physically based boundary conditions for the velocity field at the two-phase mixture swell level are stated. The system of governing equations is solved numerically with the finite volume approach for two-phase flow built in the commercial computer program. Simulations are performed for available conditions of performed physical experiments. In comparison to the previous kettle reboiler two-dimensional modeling approaches, here presented model is original regarding the applied closure laws for the interfacial friction and bundle flow resistance, as well as applied boundary conditions for the modeling of two-phase mixture free surface. Also, regarding the previous published results, here obtained numerical results are compared with the available measured data of void fraction within the tube bundle and acceptable agreement is shown.

Keywords: Kettle reboiler; Two-phase flow; Numerical simulation

1. Introduction

Reboilers are widely used in the process industry for vapour generation, while kettle reboilers are one of the most common reboiler types [1]. Also, some developments of horizontal steam generators for nuclear power plants are based on the kettle reboiler design [2]. A typical design of the kettle reboiler applied in the process industry is shown in Fig. 1. The boiling two-phase mixture flows on the shell side, across the horizontal U-tube bundle, while the heating fluid flows inside the tubes. The liquid level is controlled by a weir, so that the tube bundle is submerged. The liquid inflows on the shell side at the bottom. The gap between the bundle and the reboiler shell forms a downcomer that allows internal recirculation of liquid. The velocity of fluid across the bundle is increased by the outer recirculation of liquid, affecting the global heat transfer coefficient. The outer recirculating flow rate is proportional to the amount of generated vapour in the reboiler

$$\dot{m}_{\mathrm{in}} = C_0 \frac{\dot{Q}}{h_{\mathrm{fg}}} \tag{1}$$

where C_0 is the overflow factor and $\frac{\dot{Q}}{h_{\mathrm{fg}}}$ is the total rate of vapor generation.

Tube bundle to shell side heat transfer and thermal-hydraulic flow conditions on the shell side of the reboiler have three-dimensional character. They are determined with the tube bundle position within the reboiler shell, liquid inlet and weir positions, as well as with the mutually interconnected effects of spatial non-uniform primary to secondary side heat transfer, heat transfer and vapour

* Corresponding author. Tel.: +381 11 3370 561; fax: +381 11 3370 364.
E-mail address: estevavl@eunet.yu (V.D. Stevanovic).

0017-9310/$ - see front matter © 2005 Elsevier Ltd. All rights reserved.
doi:10.1016/j.ijheatmasstransfer.2005.10.004

Nomenclature

a	interfacial area concentration ($m^2\ m^{-3}$)
C_0	overflow factor (Eq. (1))
C_D	interfacial friction coefficient
D	diameter (m)
$\vec{G}$	mass flux vector ($kg\ m^{-2}\ s^{-1}$)
g	gravitational acceleration (ms^{-2})
h	heat transfer coefficient ($W\ m^{-2}\ K^{-1}$)
h_{fg}	latent heat of evaporation ($J\ kg^{-1}$)
$\dot{m}_k$	mass source/evaporation rate ($kg\ m^{-3}\ s^{-1}$)
$\dot{m}$	mass flow rate ($kg\ s^{-1}$)
P	tube pitch (m)
p	pressure (Pa)
$\dot{Q}$	heat power (W)
$\dot{q}_A$	heat flux ($W\ m^{-2}$)
$\dot{q}_V$	volumetric heat rate ($W\ m^{-3}$)
S	source term ($N\ m^{-3}$) surface (m^2)
$\vec{U}$	velocity vector ($m\ s^{-1}$)
V	velocity component in y direction ($m\ s^{-1}$) volume (m^3)
W	velocity component in z direction ($m\ s^{-1}$)
y, z	coordinates (m)

Greek symbols

α	volume fraction in the control volume
Δe	width of the computational cell in y or z direction (m)
ζ	pressure loss coefficient surface tension ($N\ m^{-1}$)
ρ	density ($kg\ m^{-3}$)
φ	vapour volume fraction (void) in two-phase flow
ψ	porosity

Subscripts

f	liquid
g	gas
i	interface parameter
k	phase
in	inlet
y	pertain to y direction
z	pertain to z direction
w	wall

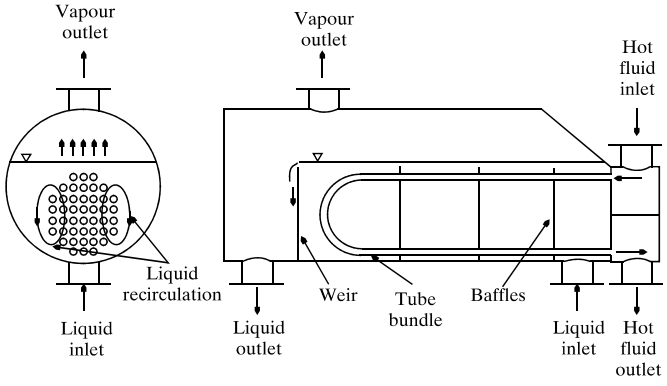

Fig. 1. Illustration of a typical kettle reboiler.

generation rate within tube bundle, inherent two-phase flow dynamics (such as liquid and vapour slip) and two-phase frictional pressure drop within tube bundles. All these conditions lead to the complex structure of freely self-organized two-phase mixture flow paths and natural circulation loops on the shell side of the kettle reboiler. Internal circulation rates and velocities of the phases are determined with multidimensional void fraction distribution and two-phase frictional pressure drop within three-dimensional geometry.

Previous investigations of the kettle reboiler shell side thermal-hydraulics have been performed with experimental and analytical models of various levels of complexity regarding the multidimensionality and thermal-hydraulic complexity of boiling two-phase flow conditions. The open literature about the kettle reboiler design and operation is relatively numerous, but here are cited only some of the papers that deal with the important problem of modeling of gas–liquid interface friction in boiling two-phase flow across tube bundles, and CFD (computational fluid mechanics) approach to kettle reboiler thermal-hydraulics. Results of one-dimensional two-phase flows across tube bundles with applications to the kettle reboiler design were reported for instance in [3–6]. The presented measured void fractions in these papers and comparisons with the homogeneous model results showed that the slip between the liquid and vapour phase flow is one of dominant effects that governs the thermal-hydraulics of two-phase flow across tube bundles. An empirical correlation was derived for the prediction of void fraction in two-phase flow across the tube bundle based on the dimensionless gas velocity [3–5]. The empirical constants in this correlation were adjusted to the applied tubes arrangement in the bundle (in-line or staggered), and to the fluid of the two-phase mixture flow (air–water and refrigerant R-113). In [6] a correlation was derived for the prediction of vapour and liquid phase slip based on the dimensionless Richardson and capillary numbers [6].

Measurements of two-dimensional void fraction distributions in two-phase flow across a circular tube bundle under different heat loads in the kettle reboiler test section were reported in [7]. The experimental bundle had 75 electrically heated tubes that provided uniform heat flux within the bundle. The tubes were arranged as one-half of a slice of a large bundle by using a vertical line of symmetry. Void fraction measurements were made by using the hot-wire anemometry. It was found that a rapid increase of the void

fraction along the bundle height occurs for heat fluxes greater than 10 kW/m^2, and the void variation in horizontal direction at certain level of the bundle was negligible. An analytical investigation of a two-dimensional upward two-phase flow across a rectangular bundle of horizontal pipes is presented in [8]. The solution of the flow was restricted to the bundle area, while the influence of the downward flow in the area between the tube bundle and the reboiler shell is taken into account through the prescribed hydrostatic pressure change at one bundle vertical side. The other vertical side is assigned to the bundle axis of symmetry and corresponding zero flow conditions in horizontal direction. The slip between the liquid and gas phase velocities was not considered and the model was applied to the conditions when the phases disengagement is not severe. Under the applied simplifications, it was shown that the flow over the bundle tubes is relatively unaffected by conditions in the shell outside area. The full CFD approach towards the kettle reboiler two-dimensional shell side thermal-hydraulics was presented in [9,10]. In both papers the two-fluid model of two-phase flow was applied, while the two-phase flow across the tube bundle was treated with the porous media approach. The importance of the gas–liquid interface friction force modeling for the proper prediction of the void fraction and velocity fields in the two-phase flow across tube bundle is emphasized in [9]. A parametric analysis of the influence of the interfacial friction on the calculated flow field was performed by applying different values of the interfacial friction coefficient, with the assumption that the prescribed constant value of this coefficient can be uniformly applied within the whole flow field regardless of the two-phase flow pattern. This crude assumption was eliminated in [10] by developing a correlation for the interfacial friction factor between the gas and liquid phases in vertical two-phase flows across in-line and staggered horizontal tube bundles. The correlation is based on the Reynolds number (calculated with the mixture density and the relative velocity between the phases), and the porosity of the tube bundle. In both papers [9,10] the upper boundary of the calculation domain was the swell level of the two-phase mixture. Its position was prescribed according to the assumed weir position and it was modeled with the constant pressure at this boundary. Also, only qualitative comparisons of the numerical results with the available measured data were done, without direct quantitative comparison and developed numerical models verification.

This paper presents a CFD approach to the simulation and analyses of the kettle reboiler shell side thermal-hydraulics. A two-dimensional two-fluid model of the kettle reboiler shell side two-phase flow across and around the tube bundle is developed. The flow across the tube bundle is based on the porous media approach. A new approach to the calculation of the gas and liquid phase interfacial friction in two-phase flow across kettle reboiler tube bundle is applied, based on modified pipe flow correlations. The tube bundle flow resistance is calculated for each phase. Two boundary conditions are applied for the modeling of the two-phase mixture swell level. The swell level is modeled with the constant pressure boundary condition, as previously done in [9,10], and with here proposed appropriate relations for the liquid and vapour phase velocities. The model is numerically solved with the commercial code and the numerical method described in [11]. Developed model is used for the simulation of one-dimensional adiabatic two-phase flow across tube bundles [3,4] and boiling two-phase flows in the kettle reboiler two-dimensional test facilities [7,12]. The obtained results are compared with the available measured data reported in [7]. The achieved agreement is satisfactory.

2. Modelling approach

Two-phase flow is simulated with a two-fluid model as two inter-penetrating continua, each having at each point in the space domain under consideration its own velocity components, enthalpy, volume fraction, density. The mathematical model consists of a system of mass and momentum conservation equations for the liquid and vapour phase. It is assumed that in boiling two-phase flow both liquid and vapour phase are saturated; hence the energy conservation equations for both phases are omitted. In order to close the system of conservative equations, laws of the interface mass and momentum transfer are defined. The following assumptions are introduced:

- Two-dimensional and steady-state conditions are simulated.
- The porous medium concept is used in the simulation of two-phase flow within tube bundles. The space of the numerical control volume can be occupied by one or both phases—vapour and liquid, as well as by tubes. The flow volume reduction due to the presence of tubes in a space occupied by a bundle is taken into account. Therefore, the conservation of vapour and liquid flow parameters is performed only for the fractions of the numerical control volume occupied by a corresponding phase.
- Tube bundle flow resistance is assumed to be continuously distributed in the space occupied by the bundle.
- Flow governing equations are written in the non-viscous form, while the turbulent viscosity effects are taken into account indirectly through friction coefficients for the tube bundles flow resistance and two-phase interfacial friction force.
- The surface tension is neglected, as it is not important for bulk two-phase flow phenomena. Hence, pressure is the same for both phases within the numerical control volume.

2.1. Governing equations

Conservation equations are written in the following form:

Mass conservation

$$\frac{\partial}{\partial y}(\alpha_k \rho_k V_k) + \frac{\partial}{\partial z}(\alpha_k \rho_k W_k) = \dot{m}_k \tag{2}$$

Momentum conservation

y-direction

$$\frac{\partial}{\partial y}(\alpha_k \rho_k V_k V_k) + \frac{\partial}{\partial z}(\alpha_k \rho_k V_k W_k) = -\alpha_k \frac{\partial p}{\partial y} - \alpha_k \rho_k g - S_{wk,y} + n S_{fg,y} + \dot{m}_k V_i \tag{3}$$

z-direction

$$\frac{\partial}{\partial y}(\alpha_k \rho_k W_k V_k) + \frac{\partial}{\partial z}(\alpha_k \rho_k W_k W_k) = -\alpha_k \frac{\partial p}{\partial z_i} - S_{wk,z} + n S_{fg,z} + \dot{m}_k W_i \tag{4}$$

Index k is f for liquid phase and g for vapour. S_{wk} represents the force of tube bundle flow resistance per unit volume exerted on phase k, and S_{fg} is the vapour and liquid phase interfacial friction force per unit volume ($n = -1$ in case of vapour phase flow and $n = 1$ in case of liquid phase flow). The mass source term due to evaporation is denoted with $\dot{m}_k$. The last term on the r.h.s. of Eqs. (3) and (4) represents momentum transfer due to evaporation, where the interface velocity is approximated with the liquid phase velocity.

It is sufficient to write only one mass balance equation (2), for instance for the liquid phase, while the other is replaced with simpler volume fraction balance equation (5).

$$\alpha_f + \alpha_g + \alpha_w = 1 \tag{5}$$

The tubes volume fraction α_w in the bundle is calculated according to Fig. 2 as

$$\alpha_w = \frac{\pi}{4}\frac{D^2}{P_y P_z} \tag{6}$$

Porosity of the tube bundle is defined as

$$\psi = 1 - \alpha_w \tag{7}$$

The vapour volume fraction in the two-phase mixture (void) is determined as

$$\varphi = \alpha_g/(\alpha_f + \alpha_g) \tag{8}$$

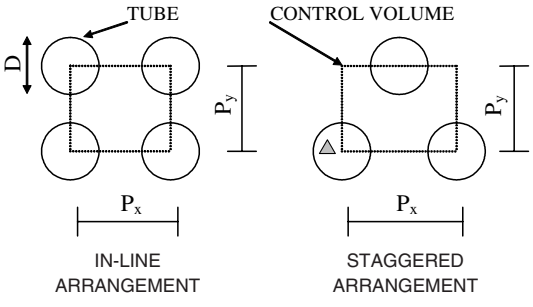

Fig. 2. Geometric parameters for a tube bundle description.

2.2. Closure laws

A variety of two-phase flow patterns can occur in a flow across a tube bundle (bubbly, churn, annular, mist [13,14]) and in a pool around the bundle (bubbly, churn, frothy [7]). Although the experimental relations between the flow parameters and two-phase flow patterns exist, they are not accompanied with corresponding models for interface transport processes that are necessary for the two-fluid model closure (such as a model for the interfacial friction). Hence, in here presented model a simple assumption about the two-phase flow patterns is applied: the bubbly flow exists for $\varphi \leqslant 0.3$, and the transitional (churn–turbulent) flow exists for $\varphi > 0.3$.

The mass source terms $\dot{m}_k$ result from mass transfer between phases by boiling.

$$\dot{m}_g = -\dot{m}_f = \frac{\dot{q}_V}{h_{fg}} \tag{9}$$

where $\dot{q}_V$ denotes the volumetric heat rate from heated walls to the liquid phase calculated with

$$\dot{q}_V = \dot{q}_A a_{iw} \tag{10}$$

where the surface heat flux $\dot{q}_A$ is specified by test conditions (in case of electrically heated tubes) or calculated with

$$\dot{q}_A = h(T_w - T_f) \tag{11}$$

and a_{iw} is the interfacial area concentration of tubes outer surface in the unit control volume

$$a_{iw} = \frac{S}{V} \tag{12}$$

where S is the tubes' outer surface within the control volume of size V. The heat transfer coefficient from a wall to a two-phase bubbly or churn–turbulent mixture is calculated with the Chen correlation as presented in [15], which is verified for many different fluids for conditions of flow boiling.

Components of the tube-fluid drag force are calculated as

$$S_{wk,e} = (1 - \alpha_w)\frac{\Delta p_{k,i}}{\Delta e} \tag{13}$$

where Δe is the width of the computational cell in y or z direction and index $k = f, g$. The pressure drop due to the two-phase mixture flow around tubes in a bundle is determined by taking into account the separate contribution of each phase to the total pressure drop. Pressure drops of liquid and vapour flows in e coordinate axis direction ($e = y, z$) are

$$\Delta p_{f,e} = \zeta_{f,e}\frac{\rho_f \hat{u}_{f,e}^2}{2}(1 - \varphi) \tag{14}$$

$$\Delta p_{g,e} = \zeta_{g,e}\frac{\rho_g \hat{u}_{g,e}^2}{2}\varphi \tag{15}$$

where $\zeta_{k,e}$, $k = f, g$ are the pressure loss coefficients in e direction, (they are calculated with the correlations

recommended in [16]). With $\hat{u}_{k,e}$ denoted is the maximum velocity of the phase k in e direction, which takes place in the clearance between tubes

$$\hat{u}_{k,e} = u_{k,e}/(1 - D/P_e) \tag{16}$$

The above Eq. (16) is derived under the assumption that the void fraction in two-phase mixture φ is uniform within the control volume.

A reliable prediction of the interfacial friction force $S_{fg,e}$ is important for a calculation of the relative velocity between vapour and liquid phase, and consequently a prediction of void fraction. Components of the interfacial drag force per unit volume of computational cell are calculated as

$$S_{fg,y} = \frac{3}{4}\alpha_g \rho_f \frac{C_D}{D_P}\sqrt{(V_g - V_f)^2 + (W_g - W_f)^2}(V_g - V_f) \tag{17}$$

$$S_{fg,z} = \frac{3}{4}\alpha_g \rho_f \frac{C_D}{D_P}\sqrt{(V_g - V_f)^2 + (W_g - W_f)^2}(W_g - W_f) \tag{18}$$

where C_D is the interfacial friction coefficient, and D_P is the diameter of the dispersed particle.

Correlations for the interfacial friction coefficient C_D are tested for flows inside tubes, while limited information is available in the literature about the prediction of C_D for two-phase flows within vertical or across horizontal tube bundles. In [17] correlations initially developed for the two-phase pipe flow are modified and successfully applied for water–steam two-phase flows across tube bundles. The same correlations are adopted here, although the flows of refrigerant R113 are simulated. For the bubbly two-phase flow across a tube bundle and in a pool around the bundle, the Ishii–Zuber correlation [18], developed for a distorted particle two-phase flow inside a tube, is adopted for the calculation of C_D

$$C_D = 0.267 D_P \left(\frac{g\Delta\rho}{\sigma}\right)^{1/2}\left\{\frac{1 + 17.67 f(\varphi)^{6/7}}{18.67 f(\varphi)}\right\}^2 \tag{19}$$

where

$$f(\varphi) = (1 - \varphi)^{1.5} \tag{20}$$

For transitional flows, a new correlation is proposed

$$C_D = 1.487 D_P \left(\frac{g\Delta\rho}{\sigma}\right)^{1/2}(1 - \varphi)^3(1 - 0.75\varphi)^2 \tag{21}$$

where the dependence on the mixture void fraction φ has the same function form as the correlation reported in [19] for the interface friction in the transitional two-phase flow patterns.

The functional dependence of the ratio C_D/D_P on the void fraction is given in Fig. 3. For transitional flow patterns, there is a rapid decrease of C_D/D_P ratio. This could be attributed to the decrease of the two-phase flow interfacial area concentration.

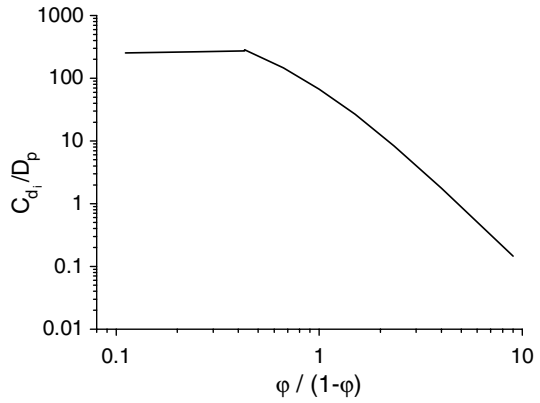

Fig. 3. Ratio of interfacial friction coefficient C_D and particle diameter D_p versus void fraction for two-phase flow across a tube bundle.

The presented model of the interfacial friction force (Eqs. (17)–(21)) are verified for the experimental tests [3,4] of adiabatic air–water two-phase flows across horizontal tube bundles with in-line and staggered arrangements of tubes. Fig. 4 shows a comparison of calculated and measured voids within the bundle. The differences between measured and predicted values are in the range of estimated uncertainties of the measured data, which is reported to be ±0.05 [3,4]. Both experimental and modelling results show void fraction dependence on two-phase flow mass flux G, as well as "S" type dependence of void on the flow quality. The increase of void fraction is saturated for the void fractions higher than 0.85. Details about here presented numerical results and comparison with experimental data are given in [17]. The same model was also successfully applied in calculation of other boiling two-phase flow conditions in nuclear steam generators and nuclear fuel assemblies [17].

2.3. Boundary conditions

The simulated flow domain on the kettle reboiler shell side is bounded by the bottom inlet, the line of symmetry on the left, the shell wall and the free surface of the two-phase mixture—the swell level that coincides with the position of the weir, as presented in Fig. 5. This flow domain is the same as in previous CFD simulations [9,10] (in [8] the flow domain was restricted only to the bundle area). The applied boundary conditions are depicted in Fig. 5. The uniform inflow of the saturated liquid is prescribed at the bottom center of the reboiler. The inflow rate is equal to the rate of vapour generation. Thus, the flow over the weir is zero and the overflow factor in Eq. (1) C_0 equals 1. This assumption is the same as in previous investigations [8–10]. At the swell level vapour separates from liquid, flows through the steam volume above the swell level and outflows at the discrete location at the reboiler's top. The recirculation of liquid at the swell level is modelled with the zero value of the liquid vertical velocity component and no change of the horizontal liquid velocity component

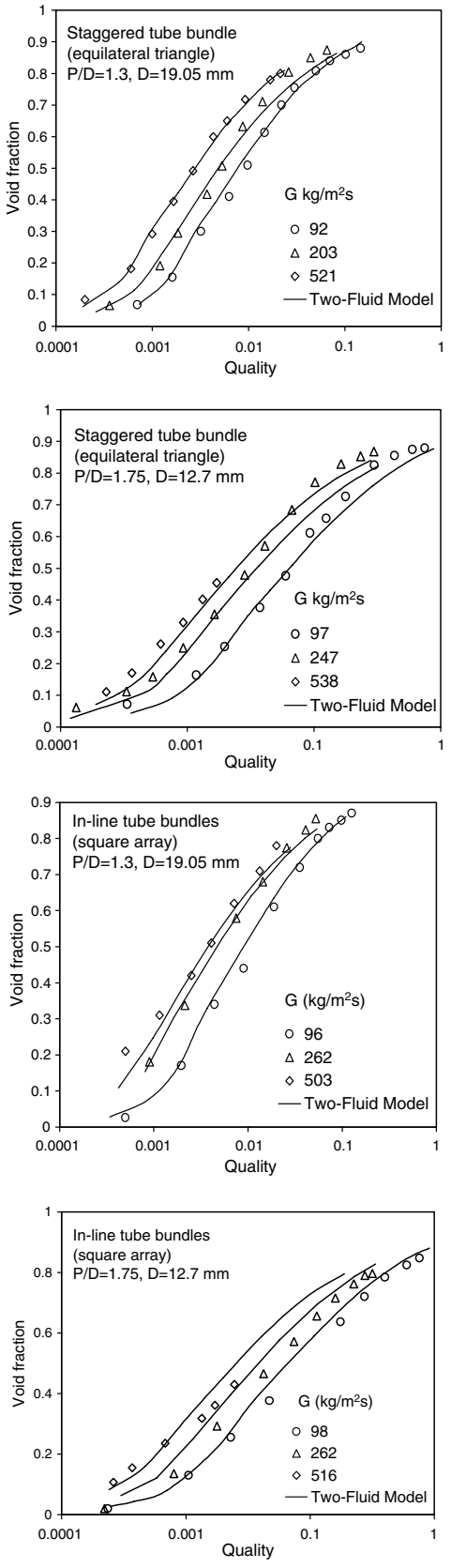

Fig. 4. Comparison of measured [4] void fraction versus flow quality and numerical simulation results for air–water flow across staggered and in-line horizontal tube bundles with different pitch to tube diameter ratios P/D.

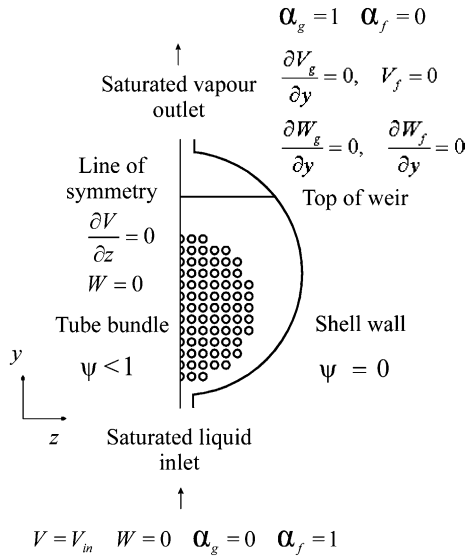

Fig. 5. Boundary conditions used in the simulation of the kettle reboiler shell side thermal-hydraulics—type I boundary conditions (type II conditions are the same except at the swell level, where the constant pressure is prescribed).

in the vertical direction, as written in Fig. 5. No change of the vapour velocity on the liquid side of the swell level is assumed. This boundary condition for the swell level is denoted as type I. Type I boundary condition is different from the condition applied in [9,10], where constant pressure at the swell level is adopted. This second boundary condition is denoted as type II. The simulations are performed with both type I and II boundary conditions at the swell level and differences in calculated flow fields are presented below. At the line of symmetry changes of all variables in horizontal direction equal zero and the horizontal velocity components of both phases equal zero. No slip condition is adopted at the shell wall. The adiabatic change of void fraction at the shell wall is applied.

3. Discretization and numerical solving

The flow field is discretized with two-dimensional control volumes as presented in Fig. 6. Two meshes shown in Fig. 6 correspond to kettle reboiler geometries with different number of tubes, which are simulated in this paper. According to the applied porous media approach, the control volume within the tube bundle is occupied with tubes and a free area filled with single phase or two-phase mixture. The shell wall is modeled with rectangular steps of inactive control volumes. The presented model is solved with the control volume based numerical method and code presented in [11]. The convergence is achieved when the sums of the absolute values of the residuals for all variables fall below 10^{-4}, which is achieved after approximately ten thousand iterations of solving of all conservative equations. Numerical mesh refinement tests have shown that the void fraction and the overall flow field predictions are

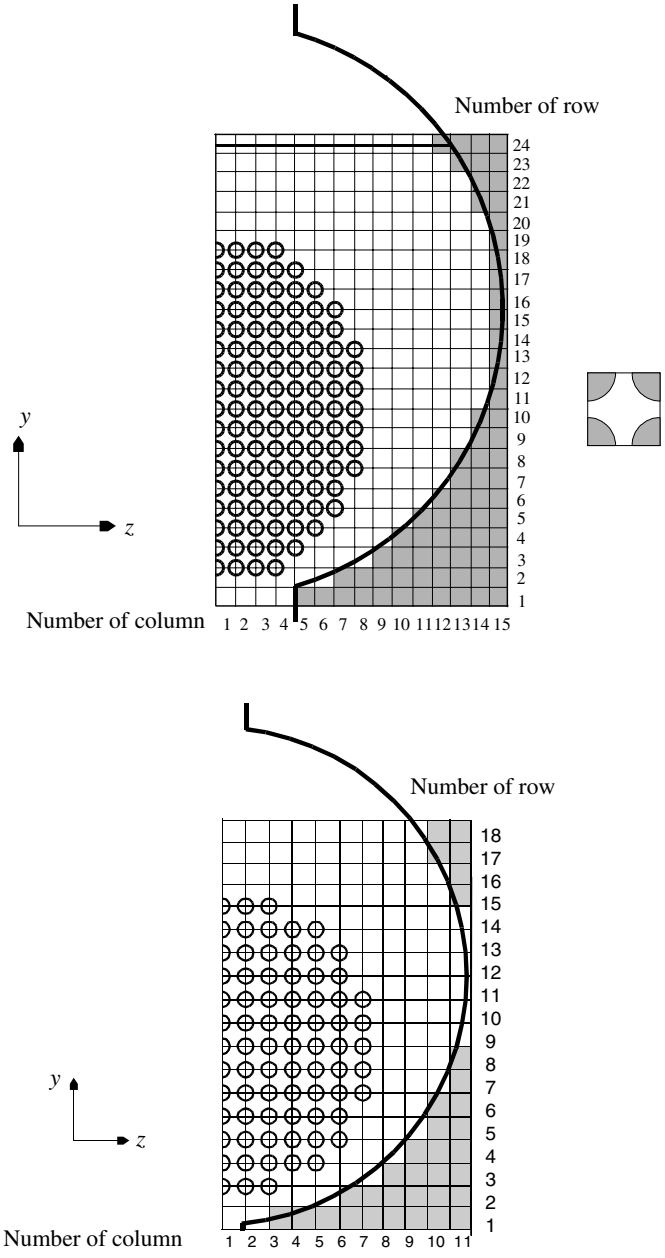

Fig. 6. Numerical meshes used in the kettle reboiler simulations: case 1 defined according to experimental conditions [9,10,12] (top), case 2 defined according to experimental conditions [7] (bottom).

relatively insensitive to the increase of the control volumes. The same was concluded in [9] with the remark that the results were affected by less than 2% with the numerical mesh refinement. Details about the computational procedure performed with the numerical code [11] are given in [20].

4. Results and discussion

Numerical simulations were preformed for two different geometries of experimental test sections as presented in Table 1 and corresponding Fig. 7. Case 1 presented in

Table 1
Geometric parameters of simulated kettle reboiler test sections (see also Fig. 7)

	Case 1 [12]	Case 2 [7]
Tube diameter $2r$	19 mm	15.9 mm
Pitch h	25.4 mm	23.85 mm
Shell radius R	0.368 m	0.254 m
Weir height from the center of shell b	0.210 m	–
Bundle center/ shell center offset a	0.114 m	0.0714 m
Number of tubes	241	75
Tubes arrangement	In-line square	In-line square
Working fluid	Refrigerant R113	Refrigerant R113

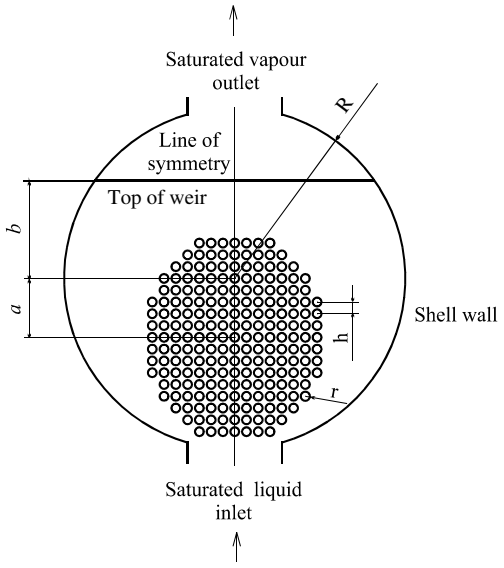

Fig. 7. Geometric parameters that define the simulated kettle reboiler test sections (corresponding values are presented in Table 1).

Table 1 corresponds to the experimental test section reported in [12], and it was later used in the CFD investigations presented in [9,10]. Measured void fraction distributions of case 2 were reported in [7]. The electrically heated tubes provided the uniform heat flux in both test sections. Experiments were performed under atmospheric pressure.

Results of the numerical simulations of case 1 are presented in Figs. 8–10. Fig. 8 shows total two-phase flow mass flux vectors calculated as

$$\vec{G} = \alpha_f \rho_f \vec{U}_f + \alpha_g \rho_g \vec{U}_g \tag{22}$$

The results in Figs. 8 and 9 are obtained with two different boundary conditions applied to the swell level modeling, type I and II, as explained in Section 2.3. Type II boundary condition was also applied in the previous CFD investigations [9,10]. The results in Figs. 8 and 9 clearly show that the swell level boundary condition considerably influences the calculated mass flux and void fraction fields. Type I boundary condition leads to the formation of one circulation

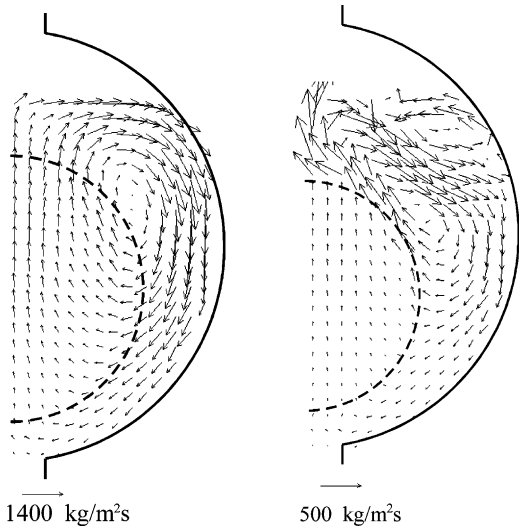

Fig. 8. Mass flux vectors of two-phase flow obtained with the swell level boundary condition of type I as presented in Fig. 5 (left) and with the constant pressure at the swell level—type II boundary condition (right); case 1 experiment (Table 1) under 20 kW/m^2.

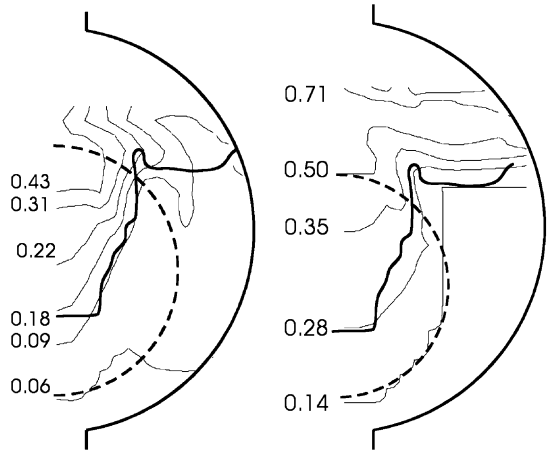

Fig. 9. Void fraction contour plots obtained with the swell level boundary condition of type I as presented in Fig. 5 (left) and with the constant pressure at the swell level—type II boundary condition (right); case 1 experiment (Table 1) under 20 kW/m^2.

centre at the boundary of the upper half of the tube bundle, as shown in the left picture in Fig. 8 (the bundle is depicted with dashed line). Strong downward flow exists in the downcomer between the bundle and the shell wall. This natural circulation is governed by the density differences between the mixture in the bundle-shell downcomer (lower void fraction and higher density) and the boiling two-phase mixture in the bundle (higher void and lower density). Results obtained with type II boundary condition for the swell level show a rather chaotic flow with at least two circulation fronts—at the boundary of the upper half of the bundle and below the swell level on the right. The flow in the lower part of the bundle-shell downcomer is less intensive than in case of type I boundary condition application. The reference

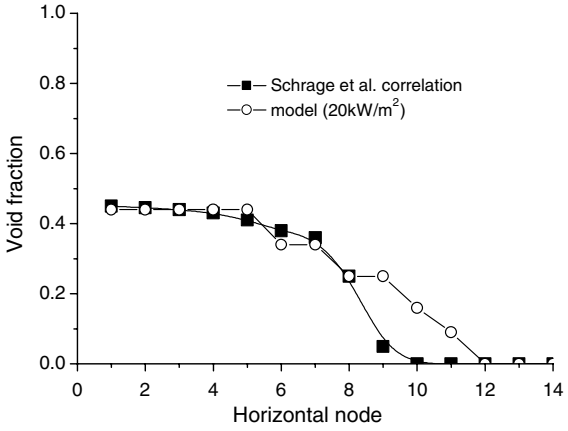

Fig. 10. Comparison of the horizontal void fraction distributions at the half of the tube bundle height calculated with the Scharge et al. model and reported in [9] and predicted with here presented two-fluid model.

mass flux vectors of 1400 kg/m^{2}s in case of type I (left picture in Fig. 8) and 500 kg/m^{2}s in case of type II boundary condition (right picture in Fig. 8) indicate less intensive overall circulation around and through the bundle in case of application of type II boundary condition. The flow field on the left picture of Fig. 8 (obtained with type I boundary condition) is similar to the flow field presented in [8] for low void flow conditions where liquid and vapour disengagement is not severe. Void fractions in the lower part of the kettle reboiler are smaller in the left picture in Fig. 9 than in the right picture. This is due to the more intensive liquid downward flow in the bundle-shell downcomer and liquid penetration from the downcomer to the bundle, as presented in the corresponding left picture in Fig. 8. The thick full line in both pictures in Fig. 9 represents the lower boundary of the region of higher void as observed in the experimental investigation [12]. The region above the full thick line is characterized as frothy. In [10] a very rapid increase in void is calculated above the dividing line with void values above 0.8 at the top of the bundle. This is not the case in here presented results. It is hardly to expect that the high values of void fraction can be achieved under considered heat flux of 20 kW/m^2. This is also supported by the measured experimental data presented for the second simulated case 2 in this paper. For heat fluxes of 10 kW/m^2 void fraction is not greater than 0.5 and for the 30 kW/m^2 not greater than 0.75. Direct void fraction and velocity field measurements do not exist for here simulated conditions of case 1 and direct verification of the numerical results is not possible; but, due to the more distinguished regions of low and high voids it is assumed that the results obtained with type I boundary condition are closer to the real process behaviour. The reasons that type II boundary condition for the swell level simulation is not consistent with the real process, and that type I boundary conditions are more reliable are clearly demonstrated with the next set of here presented numerical results of case 2. Fig. 10 shows the horizontal void fraction distributions at the half of tube bundle height calculated with the Scharge et al. empirical

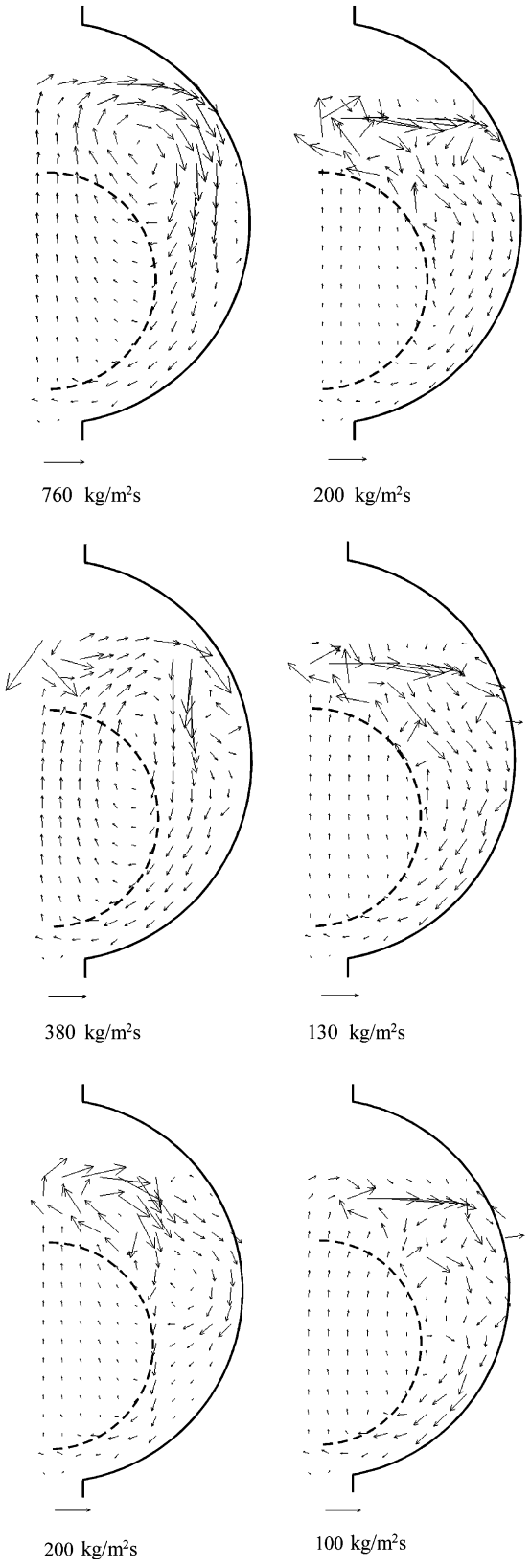

Fig. 11. Mass flux vectors of two-phase flow obtained with the swell level boundary conditions of type I as presented in Fig. 5 (left) and with the constant pressure at the swell level—type II boundary condition (right); case 2 experiment (Table 1) under 10 kW/m^2 (top), 30 kW/m^2 (middle) and 70 kW/m^2 (bottom).

correlation as reported in [9] and predicted with here presented two-fluid model. In [9] a satisfactory CFD prediction of empirically calculated void fraction presented in Fig. 10 was not achieved. In [9] the interfacial friction force in CFD approach was calculated according to the simple correlation recommended in [11]

$$S_{fg} = C_D \alpha_g (1 - \alpha_g) \rho_f \tag{23}$$

and with the constant value of the interfacial friction coefficient C_D. But, the numerical procedure could not converged for the values of $C_D < 10$ that were required in order to obtain the agreement of the CFD prediction of void fraction with the values obtained with the empirical correlation of Scharge et al. In here presented work the same commercial code is used as in [9], but no numerical problems in predicting adequate range of void fraction values is encountered. This is attributed to the here applied new model for the interfacial friction force calculation.

Numerical simulations for case 2 [7] (Table 1) are performed for three values of uniform heat fluxes across tube bundle—10 kW/m^2, 30 kW/m^2 and 70 kW/m^2. Also, type I and type II boundary conditions for the swell level are considered. The results of the total two-phase flow mass flux vectors are presented in Fig. 11. It can be seen that in both cases of applied swell level boundary conditions the recirculation mass fluxes decreases with the increase of the heat flux. In case of type I boundary condition (left pictures in Fig. 11) one recirculation center exists above the tube bundle under heat flux of 10 kW/m^2 and the whole liquid stream that outflows at the bundle top flows to the right towards the downcomer area between the bundle and the shell wall. With increase of heat flux to 30 kW/m^2 the recirculation center is moved downward to the upper right periphery of the bundle, and some part of the outflowing liquid stream at the bundle top flows towards the reboiler vertical axis of symmetry. In case with the highest heat flux of 70 kW/m^2 the recirculation from the area above the bundle to the downcomer is reduced and the more intensive recirculation is observed only in the area above the tube bundle. The results obtained with type II boundary condition (right pictures in Fig. 11) show rather chaotic flow above the tube bundle with less intensive downward recirculation in the downcomer area than the results obtained

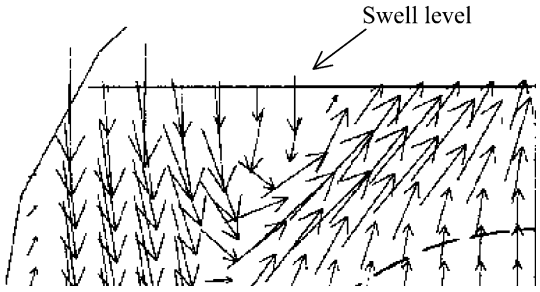

Fig. 12. Two-phase flow mass flux vectors in the vicinity of the swell level as predicted in [10] Fig. 3.

with type I boundary conditions. Also, an inconsistency in the mass flux vectors at the swell level can be observed, especially in cases for 10 kW/m^2 and 30 kW/m^2. The recirculation circles of liquid are not closed at this level and the results show that at some portion of the swell level liquid outflows, while at the rest part the swell level is a source of liquid. This can not be accepted, especially when it is assumed that the overall recirculation factor in Eq. (1) C_0 equals 1 (meaning that the liquid phase is introduced only at the reboiler bottom inlet and the total liquid flow rate equals the total evaporation rate). The same inconsistency of mass flux vector fields in the vicinity of the swell level was shown in Figs. 5, 9 and 10 in [9] and Fig. 3 in [10], where also type II swell level boundary condition was used. A detail of the numerically predicted flow filed at the swell level presented in Fig. 3 in [10] is shown here in Fig. 12. As shown with here presented results in Fig. 11, applied swell level boundary condition strongly influences the overall velocity field and recirculation rate in the kettle reboiler shell.

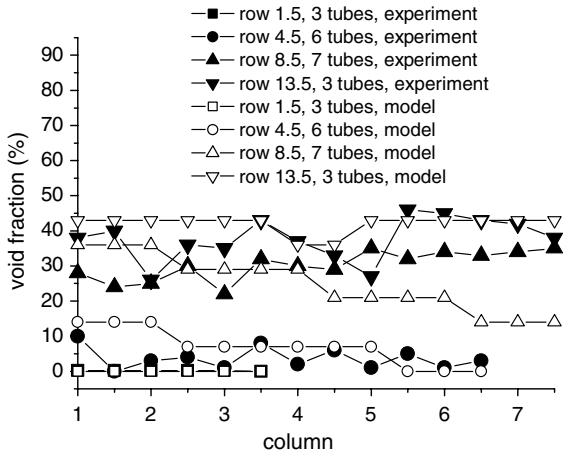

Fig. 13. Comparison with the experimental results (10 kW/m^2)—case 2 (Table 1).

Measured and calculated void fractions are shown in Figs. 13–15. Numbers of the bundle rows are shown in the bottom picture of Fig. 6. The hot-wire void measurements were taken along the horizontal directions between the rows (for instance, row 4.5 means level between 4th and 5th row). The achieved overall agreement of numerical to measured data is acceptable. The larger discrepancies

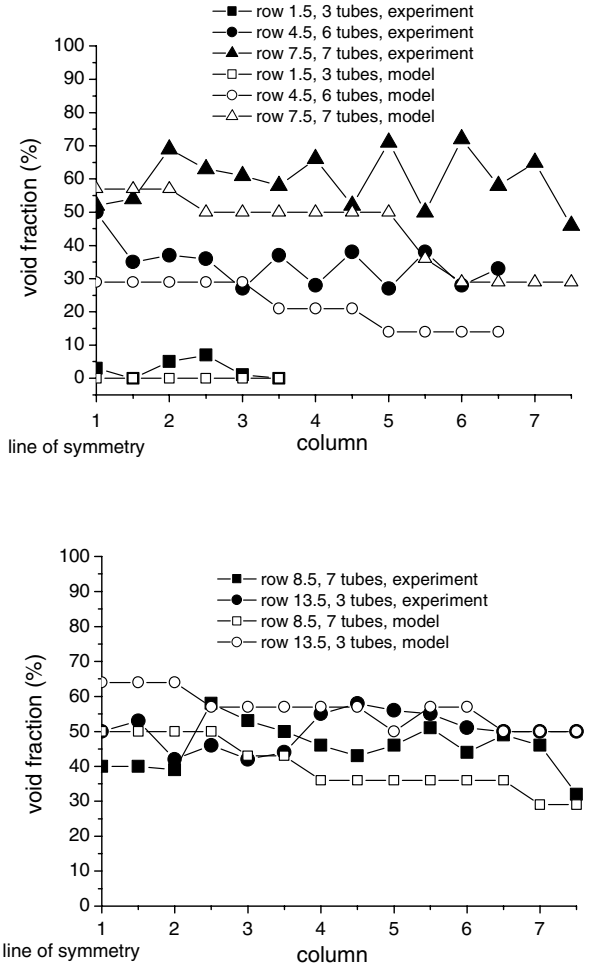

Fig. 14. Comparison with the experimental results (30 kW/m^2)—case 2 (Table 1).

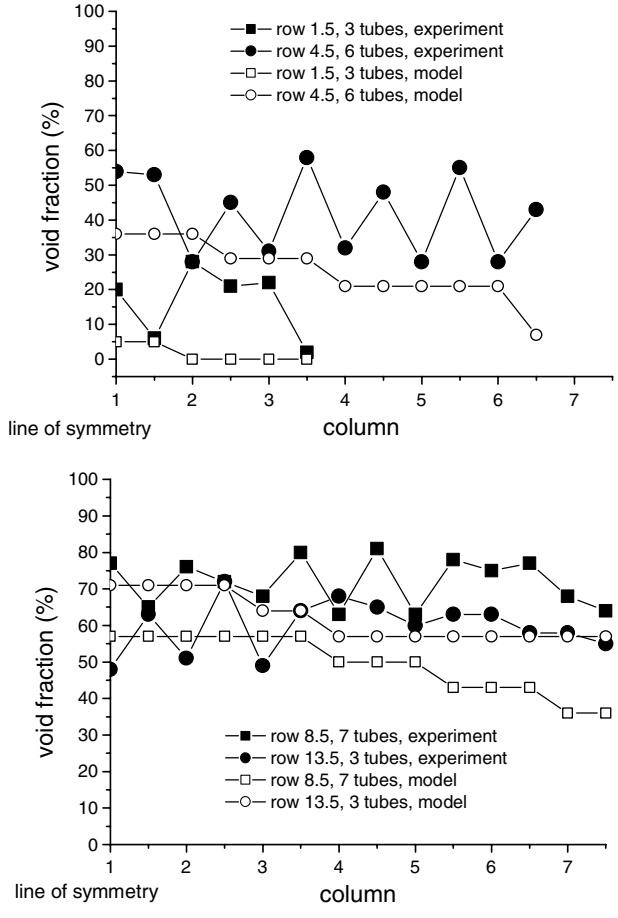

Fig. 15. Comparison with the experimental results (70 kW/m^2)—case 2 (Table 1).

are observed in the peripheral tube columns, where the penetration of the recirculating liquid from the downcomer to the bundle periphery influences the void fraction. These discrepancies are shown in Fig. 12 for row 8.5, in Fig. 13 for rows 4.5 and 7.5 and in Fig. 14 for rows 1.5, 4.5 and 8.5. The agreement is better in the inner areas of the bundle close to the axis of symmetry.

5. Conclusions

The consistent and robust two-dimensional numerical model of the kettle reboiler shell side thermal-hydraulics is presented. The new closer laws for the interfacial vapour–liquid momentum transfer due to friction Eqs. (17)–(21) and for the tube bundle flow resistance Eqs. (14)–(16) are applied. Also, the new formulation of the swell level boundary condition is introduced (as depicted in Fig. 6), which leads to the more reliable two-phase flow prediction in the vicinity of the swell level, as well as within the whole reboiler shell side. It is shown that the swell level boundary condition used in the previous investigations, based on the prescribed constant pressure at the swell level, does not lead to the consistent prediction of the flow field. In contrast to the previous CFD investigations, the obtained two-dimensional numerical predictions of the void fraction are for the first time compared with the available measured data and the overall acceptable agreement is obtained.

Acknowledgements

This work was supported by a grant from the Ministry of Science and Environmental protection of Republic of Serbia.

References

[1] P.B. Whalley, G.F. Hewitt, Reboilers, in: G.F. Hewitt, J.M. Delhaye, N. Zuber (Eds.), Multiphase Science and Technology, vol. 2, Hemisphere Publ. Co., 1986, pp. 275–331.
[2] Y. Tujikura, T. Oshibe, K. Kijima, K. Tabuchi, Development of passive safety systems for Next Generation PWR in Japan, Nucl. Eng. Des. 201 (2000) 61–70.
[3] R. Dowlati, M. Kawaji, A.M.C. Chan, Pitch-to-diameter effect on two-phase flow across an in-line tube bundle, AIChE J. 36 (1990) 765–772.
[4] R. Dowlati, A.M.C. Chan, M. Kawaji, Hydrodynamics of two-phase flow across horizontal rod bundles, J. Fluids Eng. 114 (1992) 450–456.
[5] R. Dowlati, M. Kawaji, A.M.C. Chan, Two-phase crossflow and boling heat transfer in horizontal tube bundles, J. Heat Transfer 118 (1996) 124–131.
[6] P.A. Feenstra, D.S. Weaver, R.L. Judd, An improved void fraction model for two-phase cross-flow in horizontal tube-bundles, Int. J. Multiphase Flow 26 (2000) 1851–1873.
[7] J.G. Gebbie, M.K. Jensen, Void fraction distributions in a kettle reboiler, Exp. Therm. Fluid Sci. 14 (1997) 297–311.
[8] B.M. Burnside, 2-D kettle reboiler circulation model, Int. J. Heat Fluid Flow 20 (1999) 437–445.
[9] D.P. Edwards, M.K. Jensen, A two-dimensional numerical model of two-phase heat transfer and fluid flow in a kettle reboiler, HTD-159, Phase Change Heat Transfer ASME, 1991.
[10] F.H. Rahman, J.G. Gebbie, M.K. Jensen, An interfacial friction correlation for shell-side vertical two-phase cross-flow past horizontal in-line and staggered tube bundles, Int. J. Multiphase Flow 22 (1996) 753–766.
[11] D.B. Spalding, Developments in the IPSA procedure for numerical computation of multiphase-flow phenomena with interphase slip, unequal temperatures, etc, in: T.M. Shin (Ed.), Numerical Properties and Methologies in Heat Transfer, Hemisphere Publ. Co., 1983, 421–436.
[12] K. Cornwell, N.W. Duffin, R.B. Schuller, An experimental study of the effects of fluid flow on boiling within a kettle reboiler tube bundle, ASME Paper No. 80-HT-45.
[13] A.E. Dukler, Y. Taitel, Flow pattern transition in gas–liquid systems: Measurements and modelling, in: G.F. Hewitt, J.M. Delhaye, N. Zuber (Eds.), Multiphase Science and Technology, vol. 2, Hemisphere Publ. Co., 1986, pp. 77–86.
[14] G.R. Noghrehkar, M. Kawaji, A.M.C. Chan, Investigation of two-phase flow regimes in tube bundles under cross-flow conditions, Int. J. Multiphase Flow 25 (1999) 857–874.
[15] D.C. Groeneveld, C.W. Snoek, A comprehensive examination of heat transfer correlations suitable for reactor safety analysis, in: G.F. Hewitt, J.M. Delhaye, N. Zuber (Eds.), Multiphase Science and Technology, vol. 2, Hemisphere Publ. Co., 1986, pp. 189–193.
[16] N.G. Rassohin, Nuclear Power Plants Steam Generators, second ed., Atomizdat, Moskva, 1980, pp. 112–116, (in Russian).
[17] Z. Stosic, V. Stevanovic, Advanced three-dimensional two-fluid porous media method for transient two-phase flow thermal-hydraulics in complex geometries, Numer. Heat Transfer, Part A 41 (2002) 263–289.
[18] M. Ishii, N. Zuber, Drag coefficient and relative velocity in bubbly, droplet or particulate flows, AIChE J. 25 (1979) 843–855.
[19] J.C. Rousseau, G. Houdayer, Advanced Safety Code CATHARE Summary of Verification Studies on Separate Effects Experiments, in: Proceedings of the Second International Topical Meeting on Nuclear Reactor Thermal Hydraulic-NURETH 2, Santa Barbara, USA, 1983.
[20] M. Pezo, Two-dimensional numerical simulation and analyses of the kettle reboiler shell side thermal-hydraulics, Master Thesis, University of Belgrade, 2004.